PHYSICAL REVIEW C **91**, 041601(R) (2015)

Dipolar degrees of freedom and isospin equilibration processes in heavy ion collisions

M. Papa,[1,*] I. Berceanu,[2] L. Acosta,[3] F. Amorini,[3] C. Agodi,[3] A. Anzalone,[3] L. Auditore,[4,5] G. Cardella,[1] S. Cavallaro,[3] M. B. Chatterjee,[6] E. De Filippo,[1] L. Francalanza,[3,7] E. Geraci,[1,7] L. Grassi,[1,7] B. Gnoffo,[1,7] J. Han,[3] E. La Guidara,[1] G. Lanzalone,[3,8] I. Lombardo,[9] C. Maiolino,[3] T. Minniti,[4] A. Pagano,[1] E. V. Pagano,[3,7] S. Pirrone,[1] G. Politi,[7] F. Porto,[3,7] L. Quattrocchi,[4] F. Rizzo,[3,7] E. Rosato,[9] P. Russotto,[3] A. Trifirò,[4,5] M. Trimarchi,[5,9] G. Verde,[1] and M. Vigilante[10]

[1]*INFN, Catania, Italy*
[2]*National Institute for Physics, Bucharest, Romania*
[3]*INFN-Laboratori Nazionali del Sud, Catania, Italy*
[4]*INFN, Messina, Italy*
[5]*Università facoltà di Fisica, Messina, Italy*
[6]*Saha, Institute of Nuclear Physics Kolkata, India*
[7]*Università facoltà di Fisica e Astronomia, Catania, Italy*
[8]*"Kore" Università, Enna, Italy*
[9]*Università facoltà di Fisica, Napoli, Italy*
[10]*INFN, Napoli, Italy*

(Received 23 October 2014; revised manuscript received 23 February 2015; published 8 April 2015)

The dipolar degrees of freedom on the $^{48}Ca + ^{27}Al$ system at 40 MeV/nucleon have been investigated for the first time with the 4π multidetector CHIMERA. The global variable $\langle Dz \rangle$ was measured for well-reconstructed events in binary dissipative processes. Both the close link with isospin equilibration processes and its insensitivity to later statistical hot source decays have been discussed. This latter feature provides the opportunity to investigate globally and exclusively the dynamics of the equilibration processes. At this first level of investigation the experimental evidence, supported by the study of the reference system $^{27}Al + ^{40}Ca$ and the auxiliary one $^{27}Ca + ^{48}Ca$, substantially agree with the CoMD-III calculations by describing the isovectorial forces through stiffness parameter values $\gamma \approx 0.8$–1.2.

DOI: 10.1103/PhysRevC.91.041601 PACS number(s): 25.70.−z, 21.30.Fe

The experimental evidence of heavy ion collisions highlights, in different ways, processes which evolve on different time scales. At Fermi energies, semiclassical dynamical models cannot describe the system during its overall time evolution. The observed data are usually described phenomenologically via a fast pre-equilibrium stage described using dynamical models [1–4] and later-stage processes described by statistical decay models [5]. The statistical contribution is usually separated from the dynamical one by cut-extrapolation procedures applied to angular correlation and/or to particle kinetic energy spectra (see, e.g., Refs. [6,7]). When clearly identified [8], the attempt to measure observables in principle closely linked to only one of the two regimes is therefore highly desirable. In fact, this can allow the decoupling between the effects related to the two classes of mechanisms that are linked to rather different properties of macroscopic nuclear matter. In recent decades, great efforts have been made to extract information about the nuclear isovectorial forces by studying charge-mass asymmetric systems [9–19]. The fundamental role played by the density dependence of the symmetry energy, regulated by the stiffness parameter γ, has been in fact extensively studied in recent years. This term strongly affects phenomena from nuclear structure to astrophysical processes (recent reviews include Refs. [1,2]). These attempts concern both the dynamic stage and the statistical decay of the hot sources. In particular, in this last stage the isospin and excitation energy dependencies of the level density formula play key roles and are currently under investigation [11,13,19–21].

A phenomenon closely linked to the isovectorial forces is the well-known process leading to the redistribution in momentum space of the charge-mass excess $\beta = \frac{N-Z}{A}$ [22] of the emitted particles and fragments (where Z is the charge, N is the neutron number, and A the mass number). This phenomenon, commonly referred to as the "charge-mass" or "isospin equilibration" process, is rather complex in the Fermi energy domain, especially when effects related to the finite size of the system under study have to be properly taken into account. The charge-mass distributions related to the final fragments and particles are affected by the pre-equilibrium stage (dynamical stage; explored densities different from saturation density ρ_0), which includes particle and fragment production in the midrapidity region, prompt emission, transfer of mass and charge between the main fragments, and finally particle and fragment emission from hot equilibrated sources through a multistep statistical cascade (stage with densities close to ρ_0).

As an example, in Refs. [12,17,22–24], diffusion effects on this process have been investigated by studying the isospin transport ratio obtained starting from the isotopic distributions produced near the projectile rapidity for medium-heavy symmetric or quasisymmetric systems.

In this Rapid Communication, we report on the results of investigations into the global dynamics of this equilibration process for the system $^{48}Ca + ^{27}Al$ at 40 MeV/nucleon starting from a different or complementary point of view. The

*papa@ct.infn.it

measurement was performed with the CHIMERA multidetector [25] at Laboratori Nazionali del Sud di Catania (Italy). The main goal of the experiment was to evaluate, for well-reconstructed events belonging to selected classes $\mathcal{K}$, the quantity

$$\langle \vec{D} \rangle = \left\langle \sum_{i=1}^{m} Z_i (\vec{V}_i - \vec{V}_{c.m.}) \right\rangle_{\mathcal{K}} . \quad (1)$$

The brackets indicate the average value over the ensemble $\mathcal{K}$. Z_i, V_i, m are the charges, laboratory velocities, and charged particle multiplicity of the produced particles in the selected class of events, respectively. Finally $\vec{V}_{c.m.}$ is the center of mass (c.m.) velocity. We note that in this expression the contribution of the neutral particles is implicitly contained in $\vec{V}_{c.m.}$. The interest on this quantity was triggered by two main reasons:

(i) Because of the symmetries of the statistical decay mode, $\langle \vec{D} \rangle$ is not affected by the statistical emission of all the produced sources in the later stages, as shown in Ref. [8]. This essentially happens because, due to the vectorial kinematical character of this quantity, the statistical effects are self-averaged to zero for well-reconstructed events.

(ii) As shown in Refs [8,26,27], this quantity is closely linked to the charge-mass equilibration process, because it represents the average time derivative of the total dipolar signal in the asymptotic stage (expressed in units of e).

In binary systems, for example, in the absence of dynamical neutron-proton collective motion, we have $\langle \vec{D} \rangle \equiv \vec{D}_m = \frac{1}{2}\langle \mu \rangle (\langle \beta_2 \rangle - \langle \beta_1 \rangle)(\langle \vec{V}_1 - \vec{V}_2 \rangle)$. Here, μ is the reduced mass number of the system, β_1 and β_2 are the isospin asymmetries of the two partners 1 and 2, and finally $\vec{V}_1$ and $\vec{V}_2$ are the related velocities. In the above expression, we have assumed uncorrelated fluctuations between charge-mass ratios of the partners and their relative velocity. In the other limit, the same quantity is zero if evaluated for a system represented by an equilibrated source before or after the statistical decay. As shown from dynamical microscopic calculations during a collision process between two nuclei with different charge-mass asymmetries, $|\langle \vec{D} \rangle|$ evolves over time towards smaller values in the pre-equilibrium stage. This falloff is a signal associated with the dynamics of the isospin equilibration process (see also Eq. (1) in Ref. [26]). We observe also that this change will produce a γ-ray emission through the excitation and decay of a damped dipolar dynamic mode [8,28] whose spectrum implicitly contain the time information of the process.

Therefore, $\langle \vec{D} \rangle$ is a rather well-suited global variable for selecting dynamical effects related to the isospin equilibration process. In the following, we assume that its value (normalized to $\langle |D_m| \rangle$) is a measure of the degree of isospin equilibration reached by the system due to the dynamics of the process.

The experiment was carried out by using 40 MeV/nucleon ^{48}Ca and ^{27}Al beams, at the LNS Superconducting Cyclotron. The beam impinged on $400\frac{\mu g}{cm^2}$ ^{27}Al and about $1200\frac{\mu g}{cm^2}$ ^{48}Ca,^{40}Ca targets. The chosen combinations were the following: ^{48}Ca + ^{27}Al as the main system to be investigated, ^{27}Al + ^{48}Ca as the auxiliary system (see the following), and the charge-mass quasisymmetric ^{27}Al + ^{40}Ca The charges, masses, energies, and velocities of the particles and fragments were measured with the 4π multidetector CHIMERA [25,29]. In particular, the $\Delta E - E$ technique was employed for the Z identification of fragments punching through the silicon detectors and additionally for isotopic identification of fragments with atomic numbers $Z < 10$. Mass identification was performed with the time-of-flight (TOF) technique by using the time signal from the silicon detectors with respect to the time reference of the radio-frequency signal from the cyclotron. The TOF technique is commonly used for velocity measurements of heavy ions and is also essential for the indirect determination of the mass and charge of slow TLFs (targetlike fragments) stopped in the silicon detectors. Energetic light charged particles stopped in the scintillator crystal are identified by applying the "fast-slow" discrimination method [30].

TABLE I. For different windows of Zb and for TKEL < 350 MeV, the values (cm/ns) of $\langle Dz \rangle$ and the corresponding values of $\langle Dz^D \rangle$ are shown for the ^{48}Ca + ^{27}Al system, for $\gamma = 1$.

Zb	$\langle Dz \rangle$(cm/ns)	$\langle Dz^D \rangle$(cm/ns)
12–15	− 5.73	− 5.9
15–17	− 8.36	− 8.34
17–19	− 8.86	− 8.87
20	− 9.79	− 9.78
21–22	− 5.36	− 5.30

In the following we report results collected for events with a multiplicity of detected charged particles greater than or equal to 2. We have chosen rather restrictive selection criteria to identify the "good" reconstructed events. These conditions have been prompted from calculations and have been chosen to obtain the "invariance" of the investigated quantity with respect to the statistical decay mode (see Table I). For the main system we selected events for which the total identified charge $Z^d_{\rm tot} = 33$. Checks are have been made to see whether the previous condition can be slightly relaxed, while maintaining the "invariance" condition at an acceptable level. The total detected mass cut was chosen in the interval $62 \leqslant A^d_{\rm tot} \leqslant 78$. The total measured momentum along the beam axis was selected within 70% of the theoretical value (422 amu cm/ns).

Analogous conditions have been imposed for the other systems taking into account the differences in the total mass and c.m. velocity. The well-reconstructed events have been classified according to the charge of the largest detected fragment Zb and according to the estimated total kinetic energy loss TKEL $= \mu E^{in}_A - (\sum_{i=1}^{m} \frac{1}{2} M_i V_i^2 - \frac{1}{2} M^d_{\rm tot} V^2_{c.m.,d})$. Here, E^{in}_A is the incident energy per nucleon; M_i, V_i are the measured masses and velocities; $M^d_{\rm tot}$ is the total measured mass; and $\vec{V}_{c.m.,d}$ is the related c.m. velocity associated with the detected charged particles. Therefore, each event has been also characterized through these last two quantities, which in the TKEL evaluation can globally reduce the uncertainties introduced by the imperfect mass identification and velocity

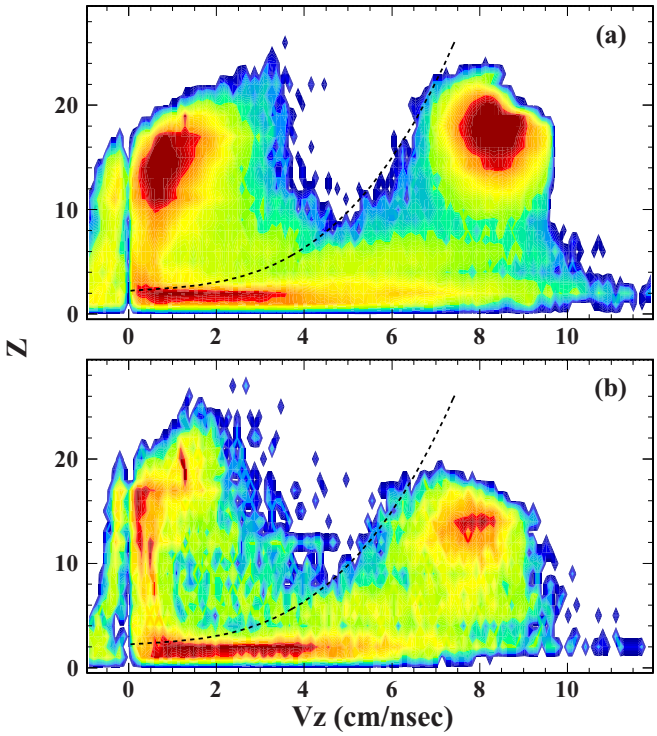

FIG. 1. (Color online) Charges Z of the detected fragments versus their velocities Vz along the beam axis are shown for the main system (a) and the auxiliary one (b).

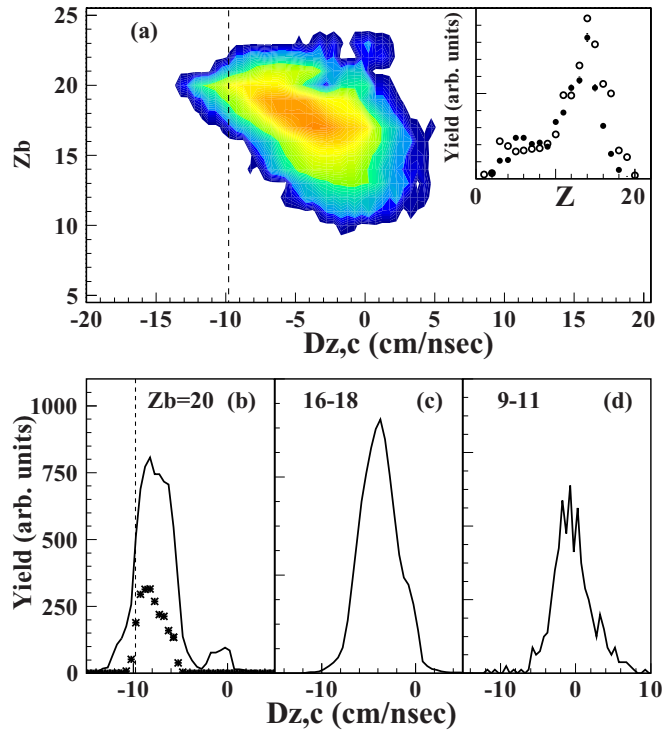

FIG. 2. (Color online) In the inset we show TKEL $<$ 350 MeV. Full dots: Charge distribution of PLF's punching through the Si detectors (direct estimate based on the $\Delta E - E$ method) for the ^{27}Al + ^{48}Ca system at 40 MeV/nucleon. Open dots: Charge distribution of TLF's stopped in the Si detectors (indirect estimate based on the TOF method) for the ^{48}Ca + ^{27}Al system at 40 MeV/nucleon. (a) For the system ^{48}Ca + ^{27}Al at 40 MeV/nucleon, the measured values of Dz,c are plotted for different Zb associated with the selected events (charged multiplicity $m \geqslant 2$). The dot-dashed vertical lines indicates the reference limiting values D_m (see the text). Panels (b)–(d): Dz,c distributions obtained as projections of the above 2-D plot, for different Zb intervals. In panel (b) the Dz,c spectra for $Zb = 20$ and for quasielastic events (TKEL $<$ 70 MeV) are plotted with star symbols.

measurement. For the main system ^{48}Ca + ^{27}Al and the auxiliary one ^{27}Al + ^{48}Ca, Fig. 1 shows the charge of the detected fragments as a function of their velocity Vz along the beam direction. In both cases, the two-dimensional (2-D) plots show the dominance of processes producing TLF's and PLF's (projectile-like fragments). The thin black curves represent the threshold of the $\Delta E - E$ charge identification technique as a function of the fragment's velocity evaluated for the typical silicon detector thickness of the CHIMERA apparatus (about 300 μm).

For each velocity value, fragments with a charge smaller than the value represented by the curves can be directly assigned by means of the $\Delta E - E$ technique. Fragments with a higher charge will be stopped in the silicon detector, the charge identification being obtained indirectly through the determination of mass obtained by means of TOF and energy measurements and by using the Charity prescription [31].

Therefore, the comparison between the TLF charge distribution obtained in the main system indirectly [see the upper portion of the Z-Vz plot in Fig. 1(a)] and the one related to the PLF for the auxiliary system assigned directly [see the lower portion of Z-Vz plot in Fig. 1(b)] allows us to highlight eventual systematic errors in the indirect charge assignment associated with the main system. The comparison has been performed for different windows of TKEL.

As shown in the inset of Fig. 2, we find that for TKEL $\lesssim$350 MeV, the charge distributions are very similar. However, some differences are observed for charges $Z \leqslant 10$. In this range, the average value of the detected charge in the direct kinematic case is larger than the inverse one, $\overline{\Delta Z} = 0.55$. This small difference is mainly due to the effects of the detection processes in the opposite kinematic conditions, which are performed with a finite geometric efficiency that also shows some asymmetries in the operating conditions between forward an backward regions. As a detailed evaluation shows, if $\overline{\Delta Z}$ is interpreted as a systematic error on the charge of these slow fragments, it produces a rather small uncertainty (less than 0.22 cm/ns) in the average dipolar signal (see Fig. 4). For the same reasons, for larger values of TKEL, the differences are instead larger making the comparison between the two cases difficult.

The present study focuses on the investigation of the dipolar component along the beam axis Z, Dz. As in the case of the TKEL determination—and to reduce eventual systematic uncertainty in the fragment velocity determination—instead of the theoretical value $\vec{V}_{c.m.}$, in Eq. (1) we use the value of $V^Z_{c.m.,d}$. $V^Z_{c.m.,d}$ is obtained event by event from the velocities along the beam axis of all the detected charged particles. We hereafter refer to this quantity as Dz,c, which represents a

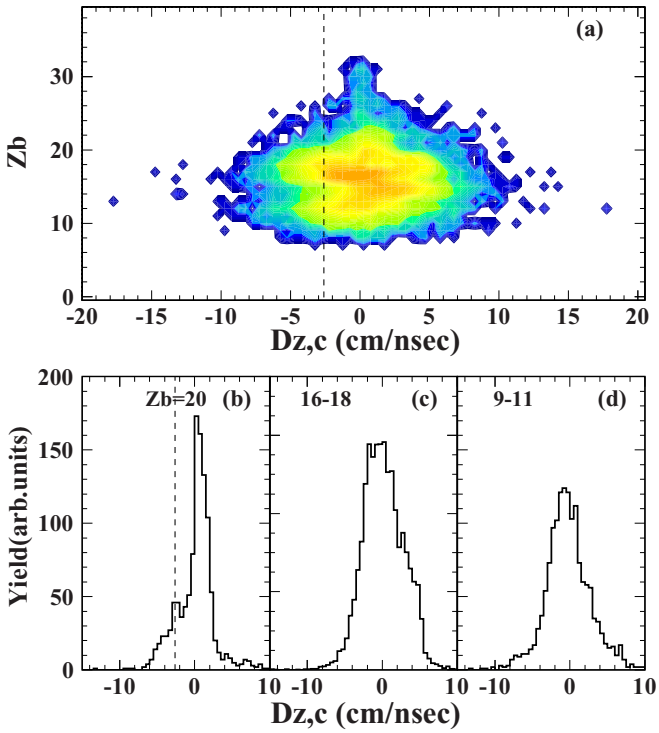

FIG. 3. (Color online) Same as in Fig. 2 but for the reference system ^{27}Al + ^{40}Ca.

partial dipolar signal related to the intrinsic motion of the subsystem formed by the charged particles. The contribution from the global relative motion of the undetected free neutrons is not included. In the following we describe a way of estimating the average total signal associated with Dz. In Fig. 2(a), we show the correlation plot of Zb vs Dz,c for the selected events of the main system. The ridge in the plot highlights an increasing trend of $\langle Dz,c\rangle$ from negative values to almost zero, for decreasing values of Zb with respect to Z_{PLF}.

We note that according to the expression given for D_m, in the initial configuration the system should exhibit a limiting value of $\langle Dz,c\rangle$ (grazing collisions) close to about -9.8 cm/ns.

The decreasing average values of $|\langle Dz,c\rangle|$, for Zb different from the projectile atomic number (i.e., less peripheral collisions), represent a clear signature of the evolution towards charge-mass equilibration. The limiting values corresponding to the most peripheral selected collisions (along the beam axis) are shown in Fig. 2 by dot-dashed vertical lines. Figures 2(b), 2(c), and 2(d) show the projections of the 2-D plot for different intervals of Zb, where we can clearly see the $\langle Dz,c\rangle$ trend. In particular, in Fig. 2(b) the spectrum with star symbols is obtained by imposing a cut of TKEL $<$ 70 MeV. The large fluctuations of Dz,c around the average value are due to physical reasons (the particular "history" of each event) and to the experimental procedure reflecting the related uncertainties. Figure 3 shows analogous plots for the reference isospin quasisymmetric system ^{27}Al + ^{40}Ca at 40 MeV/nucleon. In this case the limiting value of D_m for "grazing" collisions, is about -2.6 cm/ns and the data indeed shows values close to zero along with an enhancement near the D_m value [Fig. 3(b)].

The comparison between these systems assures us of the good level of confidence in determining $\langle Dz,c\rangle$. To obtain information about the behavior of the isovectorial interactions using this experimental data as a starting point, we have carried out CoMD-III [32,33] calculations[1] in the interval of impact parameters $b = 4$–9 fm (the weight of each b is chosen proportionally to b itself). Dynamical calculations have been followed up to about 500 fm/c. After this primary stage, the resulting main hot sources have on average an excitation energy lower than 2.5 MeV/nucelon.

For each generated event, the second stage of a multi-step statistical decay has been simulated through the Monte Carlo GEMINI code [34]. The obtained results have been analyzed with an implemented code that takes into account the main filtering effects of the experimental apparatus. This includes geometrical acceptance for the identified particles and the main selection criteria used in the analysis of experimental data.

The CoMD-III calculations have been performed for stiffness parameter values describing the isovectorial interaction, $\gamma = 0.8 (L \simeq 79$ MeV), $\gamma = 1 (L \simeq 90$ MeV), $\gamma = 1.2 (L \simeq 100$ MeV), $\gamma = 1.5 (L \simeq 114$ MeV), and symmetry energy of about 32 MeV.

According to previously investigations, the parameters of the effective Skyrme interaction corresponding to a compressibility of about 220 MeV have been chosen following Ref. [35]. Figures 4(a)–4(c) show the comparison of the calculations with the measured value of $\langle Dz,c\rangle$ (red [gray] star points), evaluated from the previously shown correlation plot in Fig. 2. The values refer to different Zb windows and TKEL $<$ 350 MeV. The vertical bars indicate the statistical uncertainty, which conservatively includes random uncertainties $\Delta Z = \pm 1$ with zero mean value on the measured fragment charges. The corresponding theoretical values are plotted in the different panels with black symbols. The comparison between the calculations and the experimental data is quantified in the figure through the "chi-square" values labelled by χ. According to this parameter, the case where $\gamma = 1$ gives the best comparison even if it is only slightly better than the case where $\gamma = 1.2$. The behavior of $\langle Dz,c\rangle$ can be understood in a qualitative way from the following remarks: As shown in the previous figure (apart from the case $\gamma = 0.8$) for $Zb < Z_{PLF}$ (dominance of mass transfer from PLF to TLF), and for $Zb > Z_{PLF}$ (onset of fusion and incomplete fusion), $\langle Dz,c\rangle$ increases: i.e., on average more charge- and mass-symmetric fragments are produced. In fact, in this case it can be verified that $\langle V^Z_{c.m.,d}\rangle \leqslant V_{c.m.}$ and therefore the c.m. of the free neutrons necessarily has to be larger than $V_{c.m.}$. This means that on average there is more neutron emission from the PLF side. The case of $\gamma = 0.8$ produces instead, for $Zb > Z_{PLF}$, a smaller value $\langle Dz,c\rangle$. In this case $\langle V^Z_{c.m.,d}\rangle \geqslant V_{c.m.}$ and therefore the cloud of neutrons has a c.m. velocity smaller than $V_{c.m.}$. In this case we have on average more neutron emission from the midrapidity and

[1]From the present study we name CoMD-III the implemented model based on the study performed in Ref. [35]. The first version, CoMD, refers to Ref. [32], while the second one, COMD-II, refers to Ref. [33].

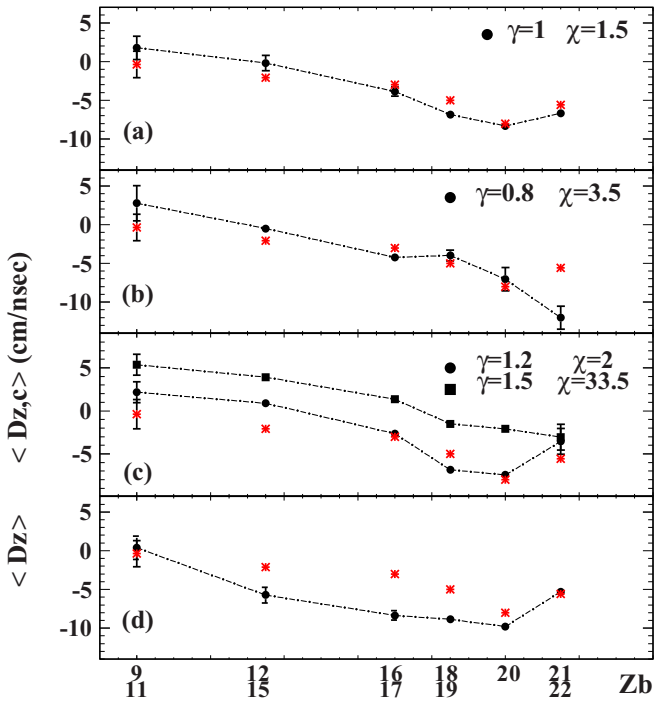

FIG. 4. (Color online) For the investigated system ^{48}Ca + ^{27}Al we plot for different Zb windows (the respective extremes are indicated by the double labeling in the Zb axis), and for TKEL < 350 MeV, the measured average dipolar signal $\langle Dz,c\rangle$ (red [gray] star points). The observed data are compared in the same figure with the results of CoMD-III + GEMINI calculations (black points), filtered through the simulated response of the experimental apparatus and data-analysis selections. Panels (a), (b), and (c) show the comparisons for different γ values characterizing the isovectorial interaction. The "chi-square" values with respect to the experimental data are also shown. (d) The calculated values of $\langle Dz\rangle$ for $\gamma = 1$ are compared to the experimental values for $\langle Dz,c\rangle$. The error bars represent statistical uncertainties due to the simulations. The estimated uncertainties related to the experimental values $\langle Dz,c\rangle$ are in many cases smaller than the plotted symbols.

TLF side. A closer look at the fragments highlights in this case a dominance of processes producing a PLF, which is only partially equilibrated in charge or mass, and an almost complete disassembly of the TLF. However, we note that this case also yields a good agreement with the experimental data for $Zb < 21$. In the region with $Zb \geqslant 21$ beyond the presence of a minor fraction of very peripheral events (not very well described by the model) we observe the onset of incomplete fusion processes. In the window $Zb = 21$–22 therefore the noticeable difference for the case $\gamma = 0.8$ could be better investigated from an experimental point of view by selecting more central collisions. Up to now we have discussed the behavior of $\langle Dz,c\rangle$ which shows a good sensitivity to the parameters of the effective interaction. To recover information about the global degree of dynamical isospin equilibration, we can evaluate $\langle Dz\rangle$ via calculations by using the same set of parameters which best fit the experimental value of $\langle Dz,c\rangle$. In Fig. 4(d), we compare the calculated values of $\langle Dz\rangle$ for $\gamma = 1$ with CoMD-III + GEMINI (including the efficiency effect), with the experimental values $\langle Dz,c\rangle$. The connection between these two quantities can be approximated by the following simple relation: $\langle Dz\rangle \cong \langle Dz,c\rangle + Z^d_{\rm tot}(\langle V^Z_{c.m.,c}\rangle - V_{c.m.})$ where $\langle V^Z_{c.m.,c}\rangle$ is the c.m. velocity for the subsystem of the charged particles. Therefore the second term in the above expression gives us an estimate of the contribution due to undetected free neutrons [36] which participate in determining the global degree of isospin equilibration. We add some observations about the "invariance" of the discussed quantities with respect to statistical decay modes. As previously observed this was shown in a rather general way in Ref. [8]. In the present work we have also checked if this insensitivity is maintained by operating with a realistic efficiency of the CHIMERA apparatus. In particular, in the analysis of the simulated data, we can retain the history of the selected primary events from the dynamical model, ordered by different Zb values, and TKEL's. It is therefore possible to evaluate the same quantity from the dynamical model $\langle Dz^D\rangle$ without taking into account the GEMINI secondary decay processes and comparing it to the value of $\langle Dz\rangle$ obtained from the complete calculations, including the efficiency effects. The calculations have been performed for different Zb windows and for TKEL < 350 MeV.

As an example, Table I shows the results for different Zb bins by using the calculations for $\gamma = 1$.

From the table we can appreciate the good agreement between the results after the GEMINI [34] de-excitation stage and the ones related to the primary events.

In summary, in the present study we have shown that the time derivative $\langle Dz\rangle$ of the total dipole related to the investigated systems represents a well-suited observable to single-out global effects associated to the dynamical stage of the isospin equilibration phenomenon. Moreover, its results are rather sensitive to the main parameter regulating the density dependence of the isovectorial forces. A next step forward in these kind of measurements would require a reliable estimation or minimization of systematic uncertainty on the velocity of the charged particles. This would permit a direct experimental estimation of $\langle Dz\rangle$, allowing also for a corresponding valuation of the global effect associated with the emitted neutrons. Longer measurements involving targets and projectiles with same charge-mass and mass asymmetry (vanishing values of $\langle Dz\rangle$ independently from the reaction mechanism) will be therefore rather useful.

Thanks are owed to C. Marchetta and E. Costa for preparing high-quality targets and also to D. Rifuggiato, L. Calabretta, and their coworkers for delivering beams with good time characteristics.

[1] B.-A. Li, L.-W. Chen, and C. M. Ko, Phys. Rep. **464**, 113 (2008), and references therein.

[2] J. M. Lattimer and M. Pakrash, Phys. Rep. **443**, 109 (2007), and references therein.

[3] V. Baran, M. Colonna, V. Greco, and M. Di Toro, Phys. Rep. **410**, 335 (2005), and references therein.
[4] A. Bonasera, F. Gulminelli, and J. Molitoris, Phys. Rep. **243**, 1 (1994).
[5] J. B. Bondorf, A. S. Botvina, A. S. Lljinov, I. N. Mishustin, and K. Sneppen, Phys. Rep. **257**, 133 (1995)
[6] S. Piantelli *et al.*, Phys. Rev. C **78**, 064605 (2008).
[7] P. Russotto *et al.*, Phys. Rev. C **81**, 064605 (2010).
[8] M. Papa *et al.*, Phys. Rev. C **72**, 064608 (2005), and references therein (see in particular Appendix D).
[9] P. Danielewicz and J. Lee, Nucl. Phys. A **922**, 1 (2014).
[10] G. Ademard *et al.*, Eur. Phys. J. A **50**, 33 (2014).
[11] G. Ademard *et al.*, Phys. Rev. C **83**, 054619 (2011).
[12] M. B. Tsang *et al.*, Phys. Rev. Lett. **92**, 062701 (2004), and references therein.
[13] P. Marini *et al.*, Phys. Rev. C **87**, 024603 (2013).
[14] Z. Kohley *et al.*, Phys. Rev. C **85**, 064605 (2012).
[15] F. Amorini *et al.*, Phys. Rev. Lett. **102**, 112701 (2009).
[16] G. Cardella *et al.*, Phys. Rev. C **85**, 064609 (2012) and references therein.
[17] Z. Chen *et al.*, Phys. Rev. C **81**, 064613 (2010).
[18] K. Brown, S. Hudan, R. T. deSouza, J. Gauthier, R. Roy, D. V. Shetty, G. A. Souliotis, and S. J. Yennello, Phys. Rev. C **87**, 061601 (2013).
[19] P. Marini, M. F. Rivet, B. Borderie, N. Le Neindre, A. Chnihi, G. Verde, and J. P. Wieleczko, EPJ Web Conf. **2**, 04003 (2010).
[20] A. Brondi *et al.*, EPJ Web Conf. **2**, 04002 (2010).
[21] S. Pirrone *et al.*, EPJ Web Conf. **17**, 16010 (2011).
[22] F. Rami *et al.*, Phys. Rev. Lett. **84**, 1120 (2000).
[23] I. Lombardo *et al.*, Phys. Rev. C **82**, 014608 (2010).
[24] Z. Y. Sun *et al.*, Phys. Rev. C **82**, 051603 (2010).
[25] A. Pagano *et al.*, Nucl. Phys. A **734**, 504 (2004); Nucl. Phys. News **22**, 25 (2012).
[26] M. Papa and G. Giuliani, J. Phys.: Conf. Ser. **312**, 082034 (2011).
[27] G. Giuliani and M. Papa, Phys. Rev. C **73**, 031601 (2006).
[28] F. Amorini *et al.*, Phys. Rev. C **58**, 987 (1998).
[29] E. De. Filippo *et al.*, Phys. Rev. C **71**, 024903 (2005).
[30] M. Alderighi *et al.*, Nucl. Instrum. Methods A **489**, 257 (2002).
[31] R. J. Charity, Phys. Rev. C **58**, 1073 (1998).
[32] M. Papa, T. Maruyama, and A. Bonasera, Phys. Rev. C **64**, 024612 (2001).
[33] M. Papa, G. Giuliani, and A. Bonasera, J. Comput. Phys. **208**, 403 (2005).
[34] R. J. Charity, D. R. Bowman, Z. H. Liu, R. J. McDonald, M. A. McMahan, G. J. Wozniak, L. G. Moretto, S. Bradley, W. L. Kehoe, and A. C. Mignerey, Nucl. Phys. A **476**, 516 (1988).
[35] M. Papa, Phys. Rev. C **87**, 014001 (2013).
[36] Z. Kohley *et al.*, Phys. Rev. C **88**, 041601 (2013).